Journal of Science and Technology – Engineering and Technology for Sustainable Development
Volume 36, Issue 2, April 2026, 044–053

Research on Establishing a Predictive Model for Surface Roughness of Al6061 Aspherical Reflector in Single Point Diamond Turning Using Back Propagation Artificial Neural Networks

Ngo Viet Hung[1], Ngo Van Tuan[2], Dao Van Duong[3], Vu Minh Hoang[4], Le Van Nhu[5], Duong Xuan Bien[1,*]

[1]*Center of Technology, Le Quy Don Technical University, Ha Noi, Vietnam*
[2] *Faculty of Mechanical Engineering, Le Quy Don Technical University, Ha Noi, Vietnam*
[3]*Faculty of Mechanical Engineering, Ho Chi Minh City University of Industry and Trade, Ho Chi Minh city, Vietnam*
[4]*Institute of Simulation Technology, Le Quy Don Technical University, Ha Noi, Vietnam*
[5]*Weapons Department, Le Quy Don Technical University, Ha Noi, Vietnam*
[*]*Corresponding author email: duongxuanbien@lqdtu.edu.vn*

Abstract

The paper presents establishing of a predictive model for surface roughness value of Al6061 material aspherical surface in ultra-precision turning using a single point diamond tool (SPDT). The model employs the structure of a back propagation artificial neural network (ANN). Three cutting parameters are considered, including spindle speed, feed rate, and depth of cut. An experimental matrix was established based on data from 30 actual experiments measuring surface roughness values of aspherical surfaces under corresponding machining conditions for the given parameter sets. Through the evaluation of six specific neural network structures (based on the number of layers and neurons in each layer), an optimal neuron ratio between layers was determined to optimize the predictive model. The ANN structure 3-5-15-1 yielded the best prediction results, as demonstrated by evaluation metrics such as: Coefficient of Determination (R^2 equal 0.9999), Mean Square Error (MSE equal 2.6e-4), Root Mean Square Error (RMSE equal 0.0163) and Mean Absolute Percent Error (MAPE equal 0.6949%).Validation experiments, involving six training sessions using MATLAB software, confirmed the high feasibility of the predictive model. This was evidenced by the minimal error (1-2%) between the predicted surface roughness values and the experimental measured roughness values. This research is directly applied to predic surface roughness value of Al6061 aspherical surface in SPDT and serves as foundation for similar studies on different material or surface geometries of machined parts.

Keywords: Aspherical Surface; artificial neural network; diamond tools; single-point diamond turning; surface roughness.

1. Introduction

The ultra-precision turning method using a diamond cutting tool, also known as Single Point Diamond Turning (SPDT), is a widely used machining technique in the production of precision mechanical components. It has emerged as a critical class of cutting processes for producing surfaces with low surface roughness and high shape accuracy [1]. Due to its advantages, SPDT is applied in the manufacturing of lens molding dies, aluminum spherical mirrors, and aspherical optical lens surfaces with various materials.

Aspherical surfaces are those that do not conform to a perfect spherical shape, meaning they do not follow the uniform curvature of a sphere. This unique geometric characteristic allows aspherical lenses to deliver improved optical performance compared to standard spherical surfaces. Aspherical surfaces are an effective solution for addressing optical aberrations and spherical errors in optical devices by concentrating light to a fine point, minimizing blurring, and enhancing image quality.

Surface roughness is a critical technical parameter because it affects the mechanical properties, wear resistance, and aesthetic appearance of the product [2-3]. The Al6061 alloy plays a vital role in advanced optical components due to its unique combination of properties, such as high strength, corrosion resistance, and good thermal insulation. Consequently, Al6061 is widely used in optical systems, where aspherical optics are preferred over spherical optics due to their higher ability to reduce astigmatism and simplify optical system design [4]. The adaptability of Al6061 material in SPDT machining of aspherical reflective mirror surfaces has been demonstrated in [5], highlighting its excellent machinability (in terms of surface roughness) after machining.

To achieve the desired surface roughness, it is essential to understand the relationship between machining parameters and their impact on surface roughness to optimize the machining process and ensure high-quality product output. Numerous studies have explored the influence of machining parameters on

p-ISSN 3093-3242
e-ISSN 3093-3579
https://doi.org/10.51316/jst.189.etsd.2026.36.2.6
Received: Apr 27, 2025; Revised: Aug 7, 2025;
Accepted: Sep 8, 2025; Online: Mar 24, 2026.

surface roughness using various predictive models, including the Response Surface Methodology (RSM), Adaptive Neuro-Fuzzy Inference System (ANFIS), and, most notably, Artificial Neural Network (ANN) models. In recent years, Artificial Neural Networks (ANNs) have garnered significant attention. With the rapid development of artificial intelligence, ANN models have been employed as effective tools for developing predictive models, outperforming other prediction models in comparative studies, as detailed in Chang's research [6]. In addition, several studies have been reviewed to demonstrate the flexibility and generalizability of the ANN model to different types of materials or machined surfaces [7-9].

Among ANN structures, the Back Propagation structure was employed in studies [10-12] to highlight the feasibility of applying back propagation neural network models to address the problem discussed here. In this paper, a method for predicting the surface roughness of aspherical surfaces made of Al6061 after SPDT machining is proposed using an ANN model. The required surface roughness data were generated, and the ANN model evaluated through experiments measuring surface roughness after machining.

During the development of the ANN model, machining parameters such as spindle speed, feed rate, and depth of cut were considered as model variables. Based on coefficients *MSE, RMSE, MAPE, and* R^2 of the experimental data, an ANN model was developed. MATLAB software was used for training and testing the neural network model. The predicted surface roughness values from the ANN model were compared with experimental results, showing a good agreement between predicted and actual values. This study demonstrates the high reliability of the ANN-based surface roughness prediction model in SPDT machining, highlighting its usefulness in reducing costs and experimental run times.

2. Research Content

2.1. Aspherical Lens and Aspherical Surface

Nowadays, aspherical lenses have become an essential component in modern technology, both in consumer markets and advanced research applications. The most notable advantage of aspherical lenses lies in their ability to compensate for spherical aberration - an optical effect in which incoming light rays converge at different focal points, resulting in image blur.

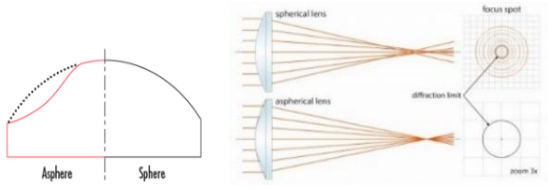

a b

Fig. 1. Aspherical surface illustration (a) and optical aberration in aspherical lenses (b)

Aspherical lenses are defined by their surface profile (sag) and are described by the formula:

$$z = \frac{Cr^2}{1+\sqrt{1-(1+K)C^2r^2}} + A_1r^2 + A_2r^4 + ... + A_8r^{16} \quad (1)$$

The formula for calculating the sag (z -height) of a spherical surface is:

$$z = \frac{Cr^2}{1+\sqrt{1-C^2r^2}} \quad (2)$$

In this study, an aspherical surface with a radius of curvature R_{as} equal 19mm was created based on the ultra-precision turning process of a spherical surface with a radius of curvature R_s equal 19.5mm using a Nanoform X diamond turning machine. This process is illustrated in Fig. 2.

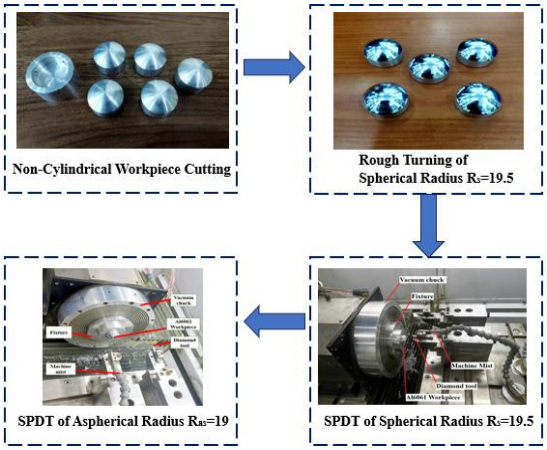

Fig. 2. Schematic diagram of machining aspherical surface workpiece

Detailed parameters of aspherical surface after machining are shown in Table 1.

Table 1. Aspherical surface parameters

Parameters	**Values**
Aspherical coefficient A_2	-7.955e-6
Aspherical coefficient A_4	1.803e-7
Aspherical coefficient A_6	-6.818e-9
Aspherical coefficient A_8	5.121e-11
Aspherical coefficient A_{10}	-1.355e-13
Aspherical radius R	19 mm
Conic constant K	0
Maximum position allowance	0.972 mm

Parameters of aspherical surfaces can be considered include surface accuracy and radius of curvature. Surface accuracy is a measure of how precisely the optical surface matches its designed shape. There are various ways to define surface accuracy and deviations from the intended surface geometry. These deviations are grouped into three categories based on their frequency on the surface of a component: form errors, waviness, and surface roughness. This study focuses on exploring the surface roughness of aspherical surfaces.

2.2. Back-Propagation Artificial Neural Network

Over the past two decades, the application of ANNs in predictive models and classification tasks has become increasingly common. Research on ANN has evolved from its inception in the 1980s to the present day, summarized by Gallo in his study [13]. ANN is inspired by the structure and functioning of biological neural systems, acting as an advanced data processing system that mirrors the complexity of human brain functions.

Structurally, ANN consists of basic computational units called neurons, which are interconnected in various architectures. A multilayer neural network architecture is illustrated in Fig. 3 and is described using input layer data, output layer data, and intermediate neurons (hidden layers) [14]. These components are tightly interconnected to form a complete neural network. This structure is designed to effectively process specific inputs. Input signals ($x_i, i = 1,2,3$) are systematically forwarded to the neurons in the hidden layer. The output layer receives activated values from the hidden layer.

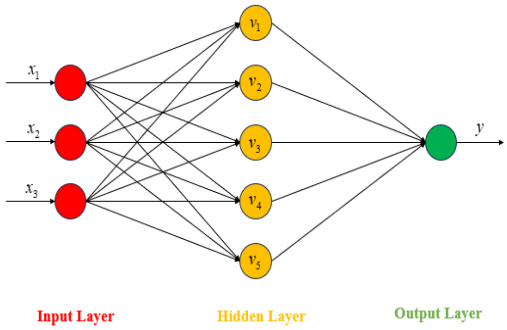

Fig. 3. Three-layer ANN architecture diagram

2.3. Establishing the Experimental Setup

The main objective of the experiment is to gather data on the surface roughness of aspherical surfaces under various machining conditions. The complete machining of the aspherical surface on the Al6061 workpiece was carried out using a Nanoform® X ultra-precision turning machine, equipped with a diamond cutting tool model NN60R0635mWGC-MS0454 (Fig. 5). All measurements of surface roughness values after SPDT were performed on 3D optical profiler ZEGAGE PRO HR (Fig. 4).

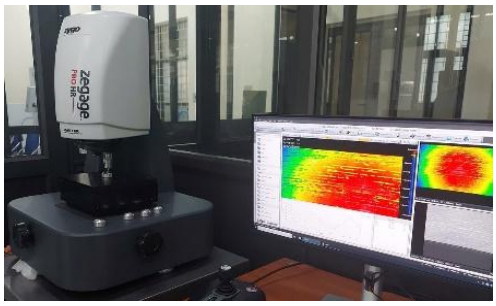

Fig. 4. The 3D optical profiler ZEGAGE PRO HR

Fig. 5. Cutting tool model NN60R0635mWGC-MS0454

Fig. 6. Aspherical workpiece

The Al6061 workpiece (Fig. 6) possesses the following geometric specifications: height (h) equal 19mm, outer diameter (ϕ) equal 30mm and spherical surface radius (R_s) equal 19.5 mm. he cutting tool parameters and chemical composition of Al6061 alloy [15] are presented in Table 2 and Table 3.

Table 2. Cutting tool specifications

Cutting edge radius	Rake angle	Cutting height	Primary Clearance	Included angle	Waviness
0.649 mm	-25°	7.475 mm	10°	60°	≤ 2 μm

Table 3. Chemical composition of Al6061

Mg	Si	Fe	Cu	Cr	Zn	Ti	Mn	Al
0.99	0.55	0.33	0.20	0.12	0.10	0.08	0.03	Balance

The SPDT process of the spherical surface of the Al6061 workpiece is illustrated in Fig. 2. The workpiece is mounted on a vacuum chuck and machined using various cutting conditions within the experimental investigation range. A high-pressure water nozzle (machine mist) is employed to remove chips from the workpiece during the machining process, ensuring the safety and integrity of the aspherical workpiece surface. After machining, the measurement of the surface roughness of the aspherical surface is conducted using the ZEGAGE PRO HR 3D optical profiler. In this experiment, the workpiece is secured on a flat support platform. An optical lens equipped with a camera moves close to the workpiece position and scans the aspherical surface (Fig. 4). Based on the positions of the interference fringes displayed on the screen, the roughness values are reviewed and compiled.

The experimental matrix presenting the results of surface roughness measurements for the aspherical surface was constructed using the Box-Behnken experimental model and the Central Composite Design (CCD). Studies [16-19] demonstrate the widespread application of these experimental models in predicting the technical parameter values of machined products. These models help reduce the number of experiments required (minimizing experimental costs) while effectively modeling the non-linear relationships between input parameters, thus enabling the precise design of predictive models. Modeling processes based on ANNs typically require a large amount of data for effective learning, as the number of parameters (weights and biases) in the neural network can be substantial. When the model includes many hidden layers and many neurons, using a small dataset can easily lead to overfitting (where the model performs exceptionally well on the training dataset but fails to generalize effectively to new data).

In this study, with an optimal set of machining parameters comprising three factors (spindle speed, feed rate, and depth of cut), the amount of data required for modeling must follow the general rule of at least 10 times the number of experiments compared to the number of model parameters. The range of values for the machining parameters is presented in Table 4. Accordingly, 30 surface roughness experiments were conducted, and the experimental results corresponding to the machining parameters of the SPDT process are detailed in Table 5.

Table 4. Technological parameter ranges

Technological parameters	Min. Value	Max. Value	Low level (-1)	Center level (0)	High. Level (+1)	Corresponding Variables
n (rev/min)	823	2177	1000	1500	2000	x_1
F (mm/min)	1.5	29	5	15	25	x_2
t (μm)	1	9	2	5	8	x_3

Table 5. Surface roughness measurements and machining conditions for 30 experiments

No.	*n* (rev/min)	*F* (mm/min)	*t* (μm)	*Ra_exp* (nm)	*Ra_pred* (nm)	*Error* (nm)	*Error* (%)
1	1000	5	5	0.99	1.00	2.11e-3	0.212
2	2000	5	5	0.90	0.90	4.35e-3	0.483
3	1000	25	5	0.81	0.81	4.60e-4	0.056
4	2000	25	5	1.08	1.08	4.40e-4	0.041
5	1000	15	2	1.47	1.47	3.00e-5	0.002
6	2000	15	2	0.88	0.88	3.05e-3	0.348
7	1000	15	8	1.62	1.62	6.48e-3	0.401
8	2000	15	8	1.44	1.45	8.08e-3	0.562
9	1500	5	2	0.79	0.79	7.10e-4	0.090
10	1500	25	2	1.30	1.30	3.20e-4	0.025
11	1500	5	8	1.52	1.52	4.27e-3	0.281
12	1500	25	8	1.46	1.45	6.37e-3	0.436
13	1500	15	5	1.02	1.01	0.01521	1.488
14	1500	15	5	1.02	1.01	0.01521	1.488
15	1500	15	5	0.98	1.01	0.02579	2.629
16	1000	5	2	2.37	2.37	8.80e-4	0.037
17	2000	5	2	1.56	1.56	9.20e-4	0.059
18	1000	25	2	1.44	1.44	5.90e-4	0.041
19	2000	25	2	2.28	2.28	2.40e-3	0.105
20	1000	5	8	1.63	1.63	1.48e-3	0.091
21	2000	5	8	1.57	1.58	6.59e-3	0.420
22	1000	25	8	1.74	1.72	0.01742	1.004
23	2000	25	8	1.52	1.52	5.27e-3	0.348
24	823	15	5	1.54	1.54	2.20e-4	0.014
25	2177	15	5	1.48	1.43	0.05267	3.559
26	1500	1.5	5	1.78	1.78	3.00e-5	0.002
27	1500	29	5	1.63	1.65	0.02058	1.263
28	1500	15	1	1.48	1.48	5.10e-4	0.034
29	1500	15	9	1.67	1.66	0.01676	1.001
30	2000	15	5	1.20	1.25	0.05272	4.408

2.4. Prediction Results and Discussion

The problem of predicting the surface roughness of aspherical surfaces involves an input layer comprising three machining parameters: cutting speed (n - rev/min), feed rate (F - mm/min), and depth of cut (t - μm). The output layer represents the predicted surface roughness value. Thus, the number of neurons in hidden layer 1 is selected as 5, aligning with the number of input variables - 3 and output variables - 1. The number of neurons in hidden layer 2 is investigated across six different ratios to evaluate the suitability and accuracy of the ANN model. Table 6 outlines the structural parameters of the ANN network.

With the number of neurons in hidden layer 1 of the neural network fixed, the ratios of neurons between the hidden layers were varied as follows: (5-5), (5-10), (5-15), (5-20), (5-25), and (5-30), corresponding to the specific structures described in Table 7. The performance of the BP network for all cases was evaluated based on specific metrics, calculated by comparing the experimental data with the predicted results. The coefficient of determination R^2 for all six ANN models is approximately equal to 1, indicating that

the predicted values from these models are highly consistent with the experimental data. The remaining accuracy metrics (*MSE, RMSE, MAPE)* highlight the differences between the predictive models, as illustrated in the bar charts shown in Fig. 7. In addition, the regression graphs illustrating the training results for each ANN structure have shown in Fig. 8.

Table 6. ANN network structure parameters

No.	ANN Model Parameters	Value
1	Number of input layer variables	3
2	Number of output layer variables	1
3	Number of first hidden layer neurons	5
4	Number of second hidden layer neurons	Tab. 7
5	Data sharing ratio: Training / Validation / Testing	80%/10%/10%
6	Number of experiments	30
7	Transfer function	poslin
8	Training function	traingdx
9	Maximum number of epochs to train	10000
10	Fitness function	*MSE*
11	Learning rate	0.01
12	Ratio to increase learning rate	1.05
13	Ratio to decrease learning rate	0.8
14	Momentum constant	0.9
15	Maximum allowable runs when the network fails to improve	6

Table 7. Structure table and calculation results of $MSE, RMSE, MAPE$, and R^2 indicators

1	R^2			*MSE*			*MAPE (%)*			*RMSE*		
	Train	**Test**	**All data**	**Train**	**Test**	**All data**	**Train**	**Test**	**All data**	**Train**	**Test**	**All data**
5-5	0.9975	0.9769	0.9945	5.2e-3	0.0525	0.0115	4.6325	12.422	5.7190	0.0724	0.2291	0.1074
5-10	0.9959	0.9987	0.9947	9.5e-3	1.5e-3	0.0112	4.5054	3.3676	5.3582	0.0973	0.0381	0.1058
5-15	0.9999	0.9999	0.9999	3.1e-4	1.9e-4	2.6e-4	0.7324	0.9874	0.6949	0.0175	0.0138	0.0163
5-20	0.9975	0.9986	0.9976	5.4e-3	3.5e-3	5.1e-3	3.3847	2.7703	3.5451	0.0737	0.0587	0.0715
5-25	0.9975	0.9955	0.9975	5.5e-3	8.4e-3	5.3e-3	2.5706	5.8104	2.6840	0.0745	0.0917	0.0727
5-30	0.9947	0.9982	0.9957	0.0106	3.8e-3	9.1e-3	5.4769	3.5568	4.9711	0.1029	0.0614	0.0952

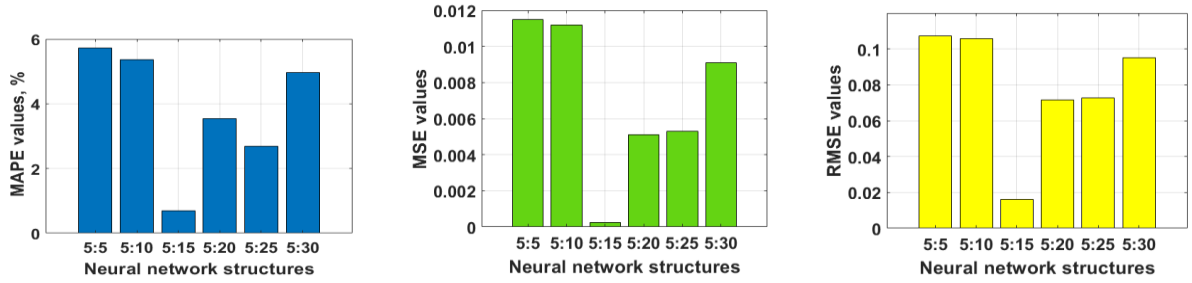

Fig. 7. *MSE*, *RMSE*, *MAPE* values corresponding to the structure ratios

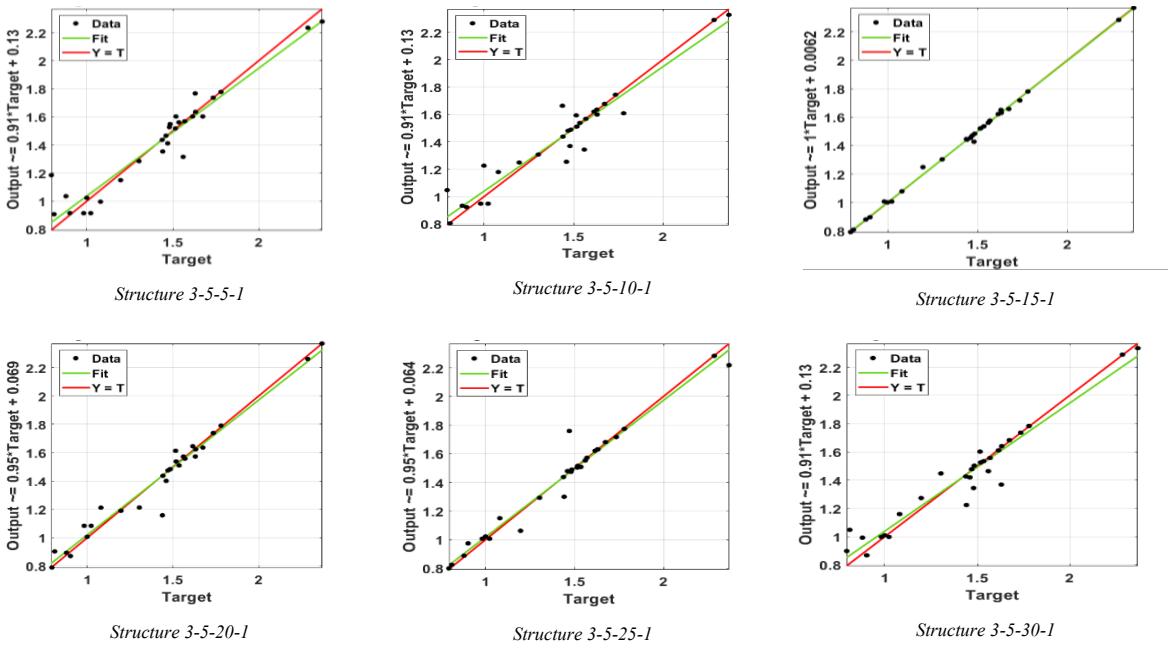

Fig. 8. Regression graphs of ANN network structures

Table 8. The R^2,*MSE, RMSE, and MAPE* andindicators of the 3-5-15-1 structure over 6 runs

NOR	R^2			*MSE*			*MAPE (%)*			*RMSE*		
	Train	**Test**	**All data**	**Train**	**Test**	**All data**	**Train**	**Test**	**All data**	**Train**	**Test**	**All data**
1	0.9999	0.9999	0.9999	3.1e-4	1.9e-4	2.6e-4	0.7324	0.9874	0.6949	0.0175	0.0138	0.0163
2	0.9998	1.0000	0.9998	4.8e-4	6.0e-5	3.9e-4	0.8665	0.4853	0.7682	0.0220	7.7e-03	0.0198
3	0.9997	0.9999	0.9998	5.6e-4	1.9e-4	5.2e-4	1.2435	0.5621	1.2020	0.0237	0.0138	0.0228
4	0.9997	0.9989	0.9996	6.4e-4	2.3e-3	8.5e-4	1.0927	2.8765	1.4032	0.0254	0.0475	0.0292
5	0.9979	0.9980	0.9980	4.8e-3	3.9e-3	4.2e-3	3.4187	2.9378	3.1536	0.0691	0.0621	0.0650
6	0.9995	1.0000	0.9996	9.0e-4	1.1e-5	7.5e-4	1.3317	0.2173	1.1644	0.0301	3.4e-03	0.0273

Through observing the above data shows that (Fig. 8): in the neural network with the structure 3-5-15-1, (corresponding to a neuron ratio of 5-15 in the hidden layers), the experimental value regression line almost coincides with the predicted value regression line from the ANN model. Moreover, the training data points are evenly distributed and closer to the regression line than the remaining structures. Based on the collected data in Table 8, the 3-5-15-1 model achieves the highest R^2 value and the lowest *MAPE, MSE, and RMSE*, demonstrating its superior prediction accuracy. The network structure 3-5-15-1 is shown in Fig. 9.

The structure of the ANN model and the number of training iterations significantly influence the training process of the back propagation network. Specifically, in each training iteration, the datasets for "Training," "Validation," and "Testing" are randomly selected at a ratio of 80%:10%:10%. This randomness leads to variations in the predictive model's results for each run. This demonstrates the objectivity of the process in constructing and selecting the network structure. The optimal dataset for the ANN structure 3-5-15-1 needs to be identified through six iterations of the predictive model, with the results of the accuracy metrics *(MAPE, MSE, and RMSE)* presented in Table 8 and Fig. 10.

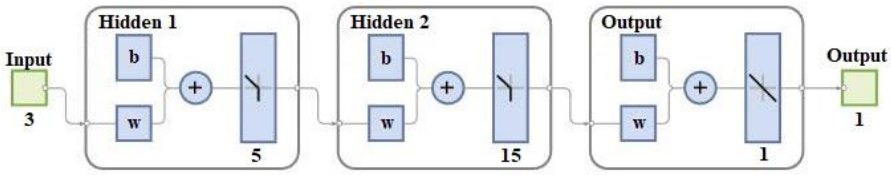

Fig. 9. The 3-5-15-1 network illustration structure

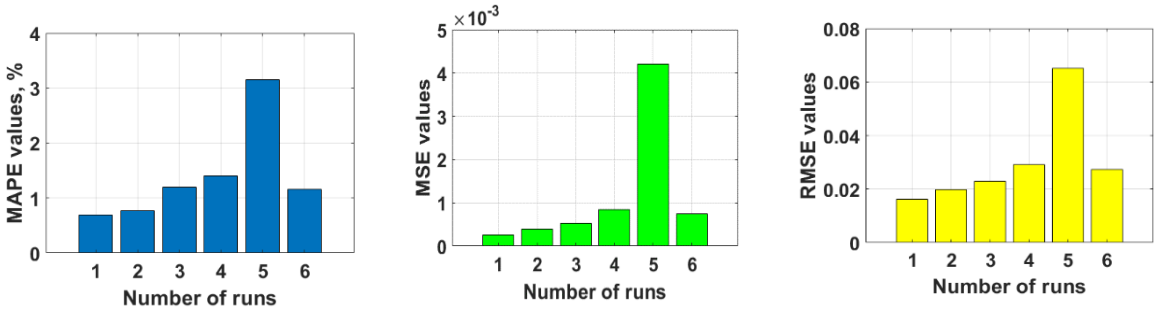

Fig. 10. *MAPE, MSE, RMSE* values corresponding to the 3-5-15-1 ANN model run order number

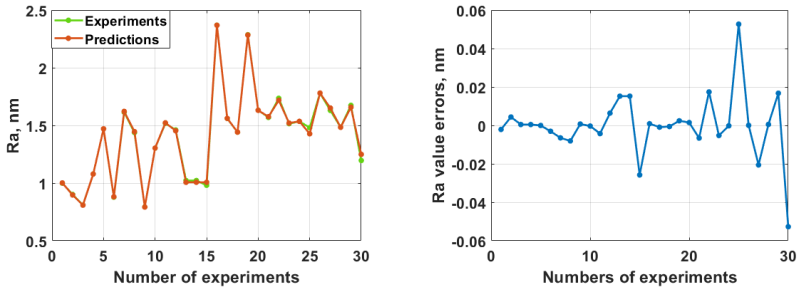

a b

Fig. 11. Comparisons of experimental and predicted surface roughness values (a) and their deviation (b)

The evaluation of the complete dataset from six iterations of the ANN model with the 3-5-15-1 structure indicates that the results from the first iteration are the most favorable. This is evidenced by the highest R^2 value of 0.9999 and the lowest values for *MAPE* equal 0.6949% , *MSE* equal $2.6e-4$ and *RMSE* equal 0.0163 compared to the other runs.

Table 5 shows the deviation (in percentage) between the predicted surface roughness values of the ANN 3-5-15-1 model from the first iteration and the experimentally measured surface roughness values. It can be observed that in most cases, the errors are very small (<1%) or small (~2%), except for the predictions in experiments 25 and 30, which exhibit relatively higher errors (>3%), reflecting the level of refinement of the predictive model. Additionally, the graph illustrating the predicted-actual surface roughness values (Fig. 11a), and the roughness error values in nanometers (Fig. 11b) is presented. It can be observed that the error values are very small and close to zero. In most cases, the predictive accuracy is exceptionally high, with deviations of less than 0.06 nm.

3. Conclusion

Overall, this study successfully developed a predictive model for the surface roughness of aspherical surfaces made of Al6061 after SPDT, based on a Back Propagation Neural Network. A dataset consisting of surface roughness measurements from 30 experiments was utilized, and six BP-ANN models were evaluated. The model with the structure 3-5-15-1, corresponding to a neuron ratio of 5-15 between the two hidden layers, was identified as the best-performing model. This structure yielded optimal evaluation metrics for the model: R^2 equal 0.9999, *MSE* equal $2.6e$-4, and *MAPE* equal 0.694%. To ensure the objectivity of the model-building and network structure selection process, the 3-5-15-1 structure was evaluated through six different training iterations using MATLAB software.

Training results indicated that in the first iteration, the roughness prediction errors between the model's predicted values and the experimentally measured roughness values were very small (1-2%).

Therefore, the predictive modeling approach presented in this study is satisfactory for forecasting surface roughness results. The ANN model demonstrates feasibility and effectiveness in reducing experimental time and cost. This research is directly applicable for predicting the surface roughness of Al6061 aspherical surfaces during SPDT machining. Additionally, it provides significant value for developing predictive models for other surface quality indicators, such as form error or other technical criteria of machined components.

References

[1] Lucca, D. A., Klopfstein, M. J., and Riemer, O., Ultra-Precision machining: Cutting with diamond tools, Journal of Manufacturing Science and Engineering, Transactions of the ASME, vol. 142, iss. 11, Oct. 2020. https://doi.org/10.1115/1.4048194

[2] Guo, J., Li, Q., Qin, P., Yuan, A., Lu, M., Ke, X., Zhang, Y., and Cheung, B. C. F., Internal surface finishing and roughness measurement: A critical review, Chinese Journal of Aeronautics, vol. 38, iss. 8, Aug. 2025, Art. no. 103303. https://doi.org/10.1016/j.cja.2024.11.013

[3] Yang, C., Su, H., Gao S., Fu Y., Ding W., and Xu J., Surface quality and geometric accuracy control of fuel nozzle single-pass honing, The International Journal of Advanced Manufacturing Technology, vol. 114, pp. 3325–3336, Apr. 2021. https://doi.org/10.1007/s00170-021-07103-5

[4] Sun, L., Duan, W., Wu, H., Chen, M., Zeng, J., Wu, Y., and Chen, Y., Investigation on the ultra-precision diamond turning of ZnSe aspheric surfaces using straight-nosed cutting tools, Journal of Manufacturing Processes, vol. 104, pp. 108–122, Oct. 2023. https://doi.org/10.1016/j.jmapro.2023.09.011

[5] Zhuang, G., Zong, W., and Tang, Y., Statistical analysis and suppression of vibration frequency bifurcation in diamond turning of Al 6061 mirror, Mechanical Systems and Signal Processing, vol. 198, Sep. 2023, Art. no. 110421. https://doi.org/10.1016/j.ymssp.2023.110421

[6] Chang, Z., Li, M., Zhu, K., Sun, L., Ye, R., Sang, M., Han, R., Jiang, Y., Li, S., Zhou, J., and Ge, R., Model predictive control of long Transfer-line cooling process based on Back-Propagation neural network, Applied Thermal Engineering, vol. 207, May 2022, Art. no. 118178. https://doi.org/10.1016/j.applthermaleng.2022.118178

[7] Dedeakayoğulları, H., Kaçal, A., and Keser, K., Modeling and prediction of surface roughness at the drilling of SLM-Ti6Al4V parts manufactured with pre-hole with optimized ANN and ANFIS, Measurement, vol. 203, Nov. 2022, Art. no. 112029. https://doi.org/10.1016/j.measurement.2022.112029

[8] Naga Malleswari, V., Kameswara Manaswy, G., and Pragvamsa, P. G., Prediction of surface roughness for fused deposition in fabricated work pieces by RSM and ANN technique, Materials Today: Proceedings, Mar. 2023. https://doi.org/10.1016/j.matpr.2023.03.378

[9] Trujillo, F. J., Martín-Béjar, S., Bañón, F., Andersson, T., and Sevilla, L., Ann-based predictive model of geometrical deviations in dry turning of AA7075 (Al-Zn) alloy, Measurement, vol. 243, Feb. 2025, Art. no. 116355. https://doi.org/10.1016/j.measurement.2024.116355

[10] Song, L., Xie, J., Jiang, Q., Wang, G., Zhong, S., Han, G., and Wu, J., A back-propagation neural network optimized by genetic algorithm for rock joint roughness evaluation, Journal of Rock Mechanics and Geotechnical Engineering, vol. 17, iss. 5, May 2025, pp. 3054–3072. https://doi.org/10.1016/j.jrmge.2024.10.022

[11] Maheshwera Reddy Paturi, U., Devarasetti, H., and Kumar Reddy Narala, S., Application of regression and artificial neural network analysis in modelling of surface roughness in hard turning of AISI 52100 steel, Materials Today: Proceedings, vol. 5, iss. 2, pp. 4766–4777. https://doi.org/10.1016/j.matpr.2017.12.050

[12] Gopal, M., Prediction of surface roughness in turning of duplex stainless steel (DSS) using response surface methodology (RSM) and artificial neural network (ANN), Materials Today: Proceedings, vol. 47, part 19, pp. 6704–6711, 2021. https://doi.org/10.1016/j.matpr.2021.05.118

[13] Gallo, C., Artificial Neural Networks Tutorial, IGI Global, Italy, pp. 6369–6378, 2014. https://doi.org/10.4018/978-1-4666-5888-2.ch626

[14] Hasan, M. M., Rahman, M. M., Islam, M. S., Chan, W. H., Alginahi, Y. M., Kabir, M. N., Bakar, S. A., and Ramasamy, D., Artificial neural network modeling for predicting thermal conductivity of EG/water-based CNC nanofluid for engine cooling using different activation functions, Frontiers in Heat and Mass Transfer, vol. 22, no. 2, pp. 537–556, 2024. https://doi.org/10.32604/fhmt.2024.047428

[15] Liu, Z., Bao, J., Hu, W., and Yan, H., Microstructure, interfacial reaction behavior, and mechanical properties of Ti3AlC2 reinforced Al6061 composites, Transactions of Nonferrous Metals Society of China, vol. 34, iss. 9, pp. 2756–2771, Sep. 2024. https://doi.org/10.1016/S1003-6326(24)66574-X

[16] Kefale Mangesha, Y., Nallamothu, R. B., Ancha, V. R., and Tesfaye Tefera, N., Optimization, production, and characterization of cottonseed methyl ester based on Box-Behnken in response surface design and gas Chromatography-Mass spectrum analysis, Energy Conversion and Management: X, vol. 23, Jul. 2024, Art. no. 100619. https://doi.org/10.1016/j.ecmx.2024.100619

[17] Emeji, I. C., and Patel, B., Box-Behnken assisted RSM and ANN modelling for biodiesel production over titanium supported zinc-oxide catalyst, Energy, vol. 308, Nov. 2024, Art. no. 132765. https://doi.org/10.1016/j.energy.2024.132765

[18] Santhosh, A. J., Tura, A. D., Jiregna, I. T., Gemechu, W. F., Ashok, N., and Ponnusamy, M., Optimization of CNC turning parameters using face centred CCD approach in RSM and ANN-genetic algorithm for AISI 4340 alloy steel, Results in Engineering, vol. 11, Sep. 2021, Art. no. 100251. https://doi.org/10.1016/j.rineng.2021.100251

[19] Ruparelia, J. R., and Patel, H. K., Harnessing the chromium reduction potential of *Pseudomonas aeruginosa JRHM33:* A comprehensive study on bioinformatics, phenotype microarray, and CCD-RSM optimization, Heliyon, vol. 10, iss. 15, Art. no. e35650. https://doi.org/10.1016/j.heliyon.2024.e35650